

# Frequency Tracking of Atrial Fibrillation using Hidden Markov Models

Frida Nilsson, Martin Stridh, and Leif Sörnmo

**Abstract**—A Hidden Markov Model (HMM) is used to improve the robustness to noise when tracking the atrial fibrillation (AF) frequency in the ECG. Each frequency interval corresponds to a state in the HMM. Following QRST cancellation, a sequence of observed states is obtained from the residual ECG, using the short time Fourier transform. Based on the observed state sequence, the Viterbi algorithm, which uses a state transition matrix, an observation matrix and an initial state vector, is employed to obtain the optimal state sequence. The state transition matrix incorporates knowledge of intrinsic AF characteristics, e.g., frequency variability, while the observation matrix incorporates knowledge of the frequency estimation method and SNRs. An evaluation is performed using simulated AF signals where noise obtained from ECG recordings have been added at different SNR. The results show that the use of HMM considerably reduces the average RMS error associated with the frequency tracking: at 5 dB SNR the RMS error drops from 1.2 Hz to 0.2 Hz.

## I. INTRODUCTION

Atrial fibrillation (AF) is a common arrhythmia, with a prevalence of over 6% for people over 80 years old [1]. The arrhythmia can be studied through the atrial activity of the surface ECG, manifested by fibrillation waves. The frequency of these fibrillation waves—the AF frequency—plays an important role when analyzing atrial fibrillation from the ECG. Several studies have demonstrated a significant correlation between the AF frequency and the likelihood of spontaneous [2] or drug-induced [3] AF termination, where a lower AF frequency indicates a higher likelihood of termination. Therefore, it is important to reliably estimate the AF frequency as it changes over time.

To study the atrial activity of the ECG, it is necessary to first cancel the ventricular activity, i.e., the QRST complexes. This task can be accomplished using various methods, including average beat subtraction methods, such as spatiotemporal cancellation [4], and source separation methods such as principal component analysis [5] and blind source separation [6].

The AF frequency has usually been obtained from the periodogram of the residual ECG, thus precluding detection of changes in AF frequency. Using the short-time Fourier transform (STFT), a frequency trend can be estimated. A more robust way to track changes in AF frequency is to make use of a spectral profile, i.e., a template of the AF spectrum [7]. Still, the residual ECG is sometimes corrupted by noise due to muscular activity or insufficient QRST cancellation. Accordingly, such noise may cause the AF frequency estimate to become unreliable.

A structured approach to handle this problem is to use a Hidden Markov Model (HMM) for frequency tracking. With an HMM, short-time frequency estimates that differ

significantly from the frequency trend can be detected and excluded or replaced by estimates based on surrounding frequencies. A Markov model consists of a finite number of states, with predefined state transition probabilities. The likelihood of a certain state depends only on the previous state (random walk). Each state corresponds to a unique set of variables which can be observed. In an HMM, on the other hand, the state variables cannot be directly observed. Each state is associated with certain observation probabilities, i.e., the probabilities of observing a specific set of variables. Given the observation sequence of an HMM, the optimal state sequence can be obtained using various algorithms such as the Viterbi or the Forward-Backward algorithm.

An HMM is well-suited for frequency tracking of a signal. The states of the model correspond to the actual frequency, while the observations correspond to the estimated frequency of a specific time interval of the signal. A priori knowledge of the likelihood by which the AF frequency changes is included in the state transition probabilities, while knowledge about the frequency estimation method and the SNR are included in the observation probabilities. HMMs have previously been applied to various radar and sonar applications, where it is of interest to track tones embedded in noise [8]–[11].

The purpose of this study is to investigate the suitability of an HMM for AF frequency tracking in ECG signals. To determine this, the method is tested on simulated AF signals mixed with noise obtained from ECG signals.

## II. METHOD

In order to use an HMM for frequency tracking, certain assumptions on the AF signal are introduced. It is assumed that changes in AF frequency are characterized by a Gaussian distribution, i.e., the AF frequency is more likely to remain the same or change gradually than to change drastically. Another assumption is that the AF frequency remains constant during the time interval in which the STFT is calculated. Yet another assumption is that the AF signal can be modeled as a sinusoidal signal with additive white noise.

Given an observed sequence,  $\mathbf{z} = [z(1), z(2), \dots, z(T)]^T$ , we want to obtain the true sequence,  $\mathbf{x} = [x(1), x(2), \dots, x(T)]^T$ . The HMM is completely characterized by a state transition matrix  $\mathbf{A}$ , an observation matrix  $\mathbf{B}$ , and an initial state vector  $\boldsymbol{\pi}$ .

When applied to frequency tracking, the  $P$  states of the HMM includes one zero-state,  $z(t) = 0$ , when no signal is present, and  $P - 1$  different frequency states,  $z(t) = 1, \dots, P - 1$ , where state  $i$  includes frequencies between  $f_i$

and  $f_i + \Delta f = f_{i+1}$ , with a center frequency of  $\tilde{f}_i$ ,

$$\tilde{f}_i = f_i + \frac{\Delta f}{2}. \quad (1)$$

#### A. State transition matrix

The  $P \times P$  state transition matrix  $\mathbf{A}$  describes the probabilities of transition between different states. Element  $a_{ij}$  is the probability that state  $x(t+1) = j$  if state  $x(t) = i$ . Each row must sum to unity, since the elements of a row correspond to the probabilities of transition to a certain state. The probability of track initialization in state  $j \neq 0$ ,  $a_{0j}$ , is set equal for each frequency state,

$$a_{0j} = \frac{u}{P-1}, \quad j = 1, 2, \dots, P-1. \quad (2)$$

Hence, the probability of remaining in the zero-state,  $a_{00}$ , i.e., when no signal is present, is

$$a_{00} = 1 - u. \quad (3)$$

The probability of track termination,  $a_{j0}$ , is equal for all frequency states,

$$a_{j0} = v, \quad j = 1, 2, \dots, P-1. \quad (4)$$

The transition probability  $\tilde{a}_{ij}$  between the non-zero states is set to

$$\tilde{a}_{ij} = \frac{(1-v)g_{ij}}{\sum_{k=1}^P g_{ik}}, \quad i, j = 1, 2, \dots, P-1, \quad (5)$$

where

$$g_{ij} = \frac{1}{d\sqrt{2\pi}} \int_{f_j}^{f_j+\Delta f} \exp\left[-\frac{(f-\tilde{f}_i)^2}{2d^2}\right] df \quad (6)$$

since the location of the frequency track at the next time step is assumed to be Gaussian with mean  $\tilde{f}_i$  and standard deviation  $d$ . This results in an unbalanced  $\mathbf{A}$ , since the diagonal elements of  $a_{ii}$  depend on state  $i$ . Hence, all diagonal elements are set to the smallest diagonal element,

$$a_{min} = \min_{1 \leq i \leq P-1} \tilde{a}_{ii}. \quad (7)$$

Consequently, the other  $P-1$  elements of the row needs to be adjusted so that the row will sum to unity. If the elements  $a_{i,i-1}$  and  $a_{i,i+1}$  becomes larger than the diagonal element of the row,  $a_{min}$ , they are set to  $a_{min}$ , and the remaining  $P-3$  elements are adjusted so that they sum to unity. This continues until no elements of the row are larger than the diagonal element  $a_{min}$ .

Using the previously described elements,  $a_{ij}$ , the design parameters of the state transition matrix  $\mathbf{A}$  are the track termination and track initiation probabilities,  $u$  and  $v$ , and the degree of frequency changes, modeled by the standard deviation,  $d$ .

#### B. Observation matrix

The  $P \times P$  observation matrix  $\mathbf{B}$  describes the probabilities of observing a specific state given the true state. The elements of  $\mathbf{B}$ ,  $b_{ij}$ , corresponds to the probability of detection in state  $j$ , when the true state is  $i$ .

We assume that the signal is a sinusoid with added noise, defined by the following signal model

$$s(n) = a \sin(2\pi f_0 n) + w(n). \quad (8)$$

The signal amplitude,  $a$ , and the frequency,  $f_0$ , is assumed to be constant over the time period where the STFT is calculated. The noise,  $w(n)$ , is assumed to be zero-mean, Gaussian with variance  $\sigma^2$ .

The probability density function of the signal magnitude  $R$  at frequency  $f$  is derived in [8]. If a sinusoid with frequency  $f$  is present, it can be expressed as

$$p_1(R(f)) = \frac{2R(f)N}{\sigma^2} \cdot I_0\left(\frac{R(f)aN}{\sigma^2}\right) \cdot e^{-\frac{N(4R(f)^2+a^2)}{4\sigma^2}}. \quad (9)$$

If absent, it can be expressed as

$$p_2(R(f)) = \frac{2R(f)N}{\sigma^2} \cdot e^{-\frac{NR(f)^2}{\sigma^2}}, \quad (10)$$

where  $N$  defines the length of the Fourier transform, and  $I_0$  is the modified Bessel function.

The elements of the observation matrix  $\mathbf{B}$  are derived from  $p_1$  and  $p_2$ . If no signal is present, the probability of no detection (zero-state),  $b_{00}$ , and the probability of detection in state  $i$ ,  $b_{0i}$ , is

$$b_{00} = \prod_{i=1}^{P-1} \int_0^D p_2(r) dr = \left[1 - e^{-\frac{D^2 N}{\sigma^2}}\right]^{P-1}, \quad (11)$$

$$b_{0i} = \frac{1 - b_{00}}{P-1}, \quad (12)$$

where  $D$  is the detection threshold.

If a signal with frequency between  $f_m$  and  $f_m + \Delta f$  is present, the probabilities of detection in state  $m$ ,  $b_{mm}$ , no detection (zero-state),  $b_{m0}$ , and detection in state  $i \neq m$ ,  $b_{mi}$  are given by

$$b_{mm} = \int_D^\infty p_1(r) \cdot \left[1 - e^{-\frac{r^2 N}{\sigma^2}}\right]^{P-2} dr, \quad (13)$$

$$b_{m0} = \left[1 - e^{-\frac{D^2 N}{\sigma^2}}\right]^{P-2} \int_0^D p_1(r) dr, \quad (14)$$

$$b_{m,i \neq m} = \frac{1 - b_{m0} - b_{mm}}{P-2}, \quad (15)$$

respectively.

The design parameters of  $\mathbf{B}$  is the SNR, given by the parameters  $a$  and  $\sigma^2$ , and the detection threshold,  $D$ .

#### C. Optimal detection threshold

An optimal detection threshold,  $D_{opt}$ , can be obtained if the following error cost function criterion is used,

$$C_e = \alpha P(R_1 > D \cap \dots \cap R_P > D | i = 0) + \beta P(R_1 < D \cup \dots \cup R_P < D | i \neq 0) \quad (16)$$

where the sum of  $\alpha$  and  $\beta$  equals 1. Setting the derivative of  $C_e$  to zero, one obtains an expression of the probability of a magnitude equal to the detection threshold,  $D$ , when a signal is present:

$$p_1(D) = \frac{2DN(P-1)\alpha\mu_0}{\sigma^2\beta(1-\mu_0)} e^{-\frac{D^2N}{\sigma^2}} \left(1 - \frac{\beta(1-\mu_0)(P-2)b_{0i}}{\alpha\mu_0(P-1)b_{00}}\right), \quad (17)$$

where  $\mu_0$  is the long term probability of the zero-state.

By setting  $\alpha = (1 - \mu_0)$  and  $\beta = \mu_0$ , false dismissals are emphasized if the probability of being in the zero-state is small, and vice versa. This gives

$$p_1(D) = \frac{2DN(P-1)}{\sigma^2} e^{-\frac{D^2N}{\sigma^2}} \left(1 - \frac{(P-2)b_{i0}}{(P-1)b_{00}}\right). \quad (18)$$

The optimal threshold,  $D_{opt}$ , is then

$$D_{opt} = \arg \max_D p_1(D). \quad (19)$$

Since  $b_{i0}$  and  $b_{00}$  depends on  $D$ ,  $D_{opt}$  has to be calculated iteratively. By using the cost function optimality criterion, the only design parameters of  $\mathbf{B}$  are  $a$  and  $\sigma^2$ .

### III. EVALUATION AND RESULTS

#### A. Signals and parameter values

The HMM method was evaluated using simulated AF signals. To investigate the robustness of the method, real noise was added. The AF signals are simulated as a sinusoid, with varying amplitude, fundamental frequency and its  $M$  harmonics [4]:

$$s(n) = - \sum_{i=0}^{M-1} a_i(n) \sin(i\theta(n)), \quad (20)$$

where  $a_0$  and  $a_i, i = 1, \dots, M$ , are the amplitudes of the fundamental and the harmonics, respectively, and  $\theta(n)$  is the phase.

The time varying amplitude  $a_i(n)$  of the  $i$ :th harmonic is given by

$$a_i(n) = e^{-\gamma i} (a + \Delta a \sin(2\pi \frac{F_a}{F_s} n)), \quad (21)$$

where the amplitude  $\Delta a$  is the modulation peak amplitude and  $F_a$  is the modulation frequency. The exponential decay of the amplitudes of the harmonics is denoted  $\gamma$ .

The fundamental AF frequency varies around  $F_0$  with maximum frequency deviation of  $\Delta F$  and a modulation frequency  $F_m$ . Hence, the phase is given by

$$\theta(n) = 2\pi \frac{F_0}{F_s} n + \frac{\Delta F}{F_m} \sin(2\pi \frac{F_m}{F_s} n). \quad (22)$$

The signal amplitude is set to  $a = 100$  and the modulation amplitude and frequency is set to  $\Delta a = 30$  and  $F_a = 0.08$ , respectively. AF signals with four different frequency trends were created: constant frequency, varying frequency, gradually decreasing frequency and stepwise decreasing frequency. The frequency trends of the simulated signals are shown in Fig. 1.

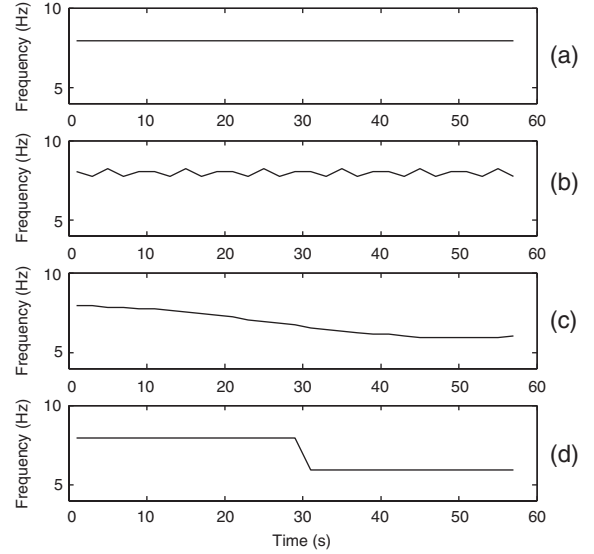


Fig. 1. Frequency trends of the simulated AF signal with (a) constant frequency, (b) varying frequency, (c) gradually changing frequency and (d) stepwise changing frequency.

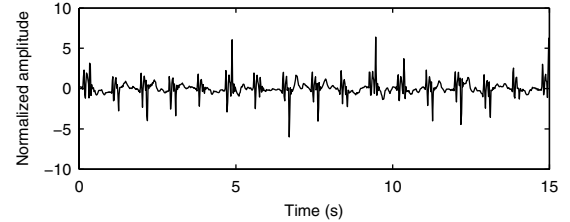


Fig. 2. Noise obtained from ECG signal.

Noise, present in ECG signals, was added to the simulated AF signals. In order to acquire the noise signal, QRST complexes was removed from ECG signals with normal sinus rhythm, using average beat subtraction. Figure 2 shows the noise signal.

The SNR is defined by

$$SNR = 20 \log \frac{V_x}{\sigma_v} \quad (23)$$

where  $V_x$  is the peak-to-peak amplitude of the simulated AF signal, and  $\sigma_v$  is the standard deviation of the noise. Test signals with SNR between 0 dB and 10 dB was created. Figure 3 shows a simulated AF signal with added noise at 5 dB SNR.

The frequencies between 3 and 12 Hz are divided into segments of  $\Delta f = 0.1$  Hz, so that state 1 contains frequencies between 3 and 3.1 Hz, and so on until state  $P$  with frequencies between 11.9 and 12 Hz. This gives a total of  $P = 91$  states, including the zero-state.

Since absence of fibrillation is assumed to be unlikely, the track initiation probability is set to  $u = 0.98$  and the track termination probability is set to  $v = 0.01$ . The standard deviation is set to  $d = 0.5$ .

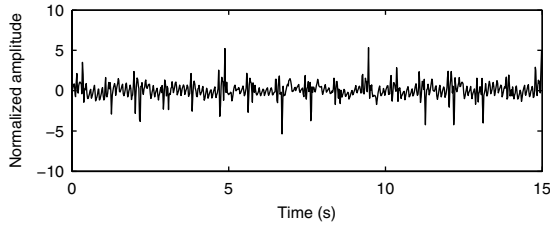


Fig. 3. Simulated AF signal mixed with noise to 5 dB SNR. The resulting signal represents the case where QRST cancellation cannot be accurately performed.

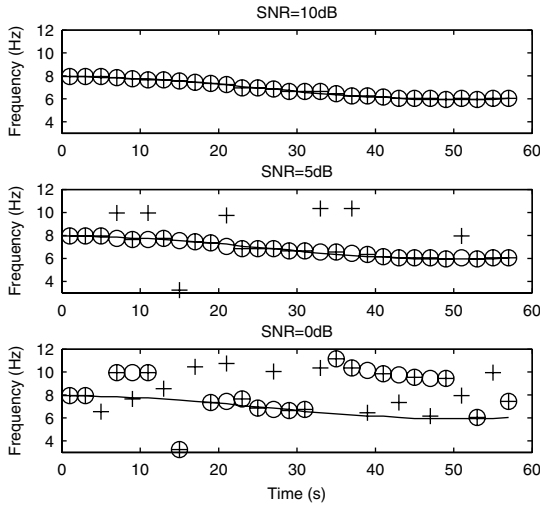


Fig. 4. Frequency tracking with and without employing the HMM of simulated AF signals mixes with QRST-noise to different SNR. Solid line shows the actual frequency trend, '+' the estimated frequency of the mixed signal, and 'o' the estimated frequency of the mixed signal using HMM.

The signal and noise amplitudes of the observation matrix  $\mathbf{B}$  are set to  $a = 0.1$  and  $\sigma^2 = 0.1$  respectively. Note that the HMM is not matched to the simulation model.

### B. Results

An example of HMM frequency tracking is presented in Fig. 4. The HMM improves the frequency tracking performance at SNRs ranging from 9 down to 0 dB. For signals with very high SNR the spectral peaks can be clearly distinguished. Hence, the observed states equal the true states, and there is no need to employ the HMM. For signals with very low SNR, where the observed frequencies are so corrupted by noise that no observed state is equal to the true state, the frequency tracking cannot be improved by the HMM.

The average RMS error of the estimated frequencies, obtained with and without the HMM, is presented in Fig. 5. For example, the average RMS error drops from 1.2 to 0.2 Hz, when the HMM is applied at 5 dB SNR. When the optimal state, given by the Viterbi track, is the zero-state, the error is undefined. A high zero-state occupancy percentage tend to give a lower average RMS error. Therefore it is important to compare not only the average RMS error, but

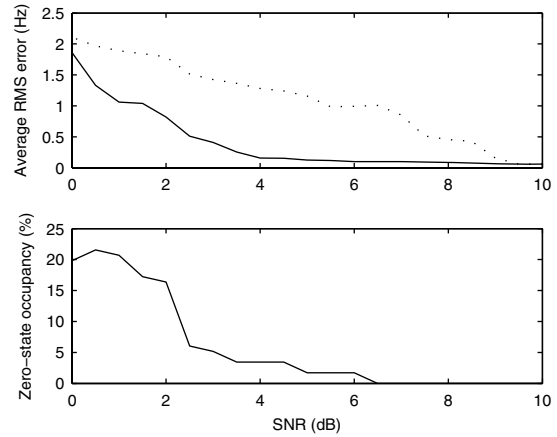


Fig. 5. RMS error and zero-state occupancy as function of SNR. (Top) solid line shows RMS error using HMM, while dotted lines shows RMS error when no HMM was employed. (Bottom) Zero-state occupancy when using HMM.

also the zero-state occupancy percentage.

The results suggests that the assumption of white noise in the HMM is not crucial, since the performance for colored noise is good.

## IV. CONCLUSIONS

Frequency tracking with HMM was evaluated using simulated AF signals with varying amplitude and frequency embedded in noise obtained from ECG recordings, showing that HMM improves the frequency tracking substantially.

## REFERENCES

- [1] V. Fuster *et al.*, "ACC/AHA/ESC guidelines for the management of patients with atrial fibrillation," *Circ.*, vol. 104, pp. 2118–2150, 2001.
- [2] F. Nilsson, M. Stridh, A. Bollmann, and L. Sörnmo, "Predicting spontaneous termination of atrial fibrillation with time-frequency information," *Computers in Cardiology*, vol. 31, pp. 657–660, 2004.
- [3] A. Bollmann, N. Kanuru, K. McTeague, P. Walter, D. B. DeLurgio, and J. Langberg, "Frequency analysis of human atrial fibrillation using the surface electrocardiogram and its response to ibutilide," *Am. J. Cardiol.*, vol. 81, pp. 1439–1445, 1998.
- [4] M. Stridh and L. Sörnmo, "Spatiotemporal QRST cancellation techniques for analysis of atrial fibrillation," *IEEE Trans. Biomed. Eng.*, vol. 48, no. 1, pp. 105–111, 2001.
- [5] P. Langley, J. P. Bourke, and A. Murray, "Frequency analysis of atrial fibrillation," *Computers in Cardiology*, vol. 27, pp. 65–68, 2000.
- [6] J. J. Rieta, V. Zarzoso, J. Millet-Roig, R. Garcia-Civera, and R. Ruiz-Granell, "Atrial activity extraction based on blind source separation as an alternative QRST cancellation for atrial fibrillation analysis," *Computers in Cardiology*, vol. 27, pp. 69–72, 2000.
- [7] M. Stridh, L. Sörnmo, C. J. Meurling, and S. B. Olsson, "Sequential characterization of atrial tachyarrhythmias based on ECG time-frequency analysis," *IEEE Trans. Biomed. Eng.*, vol. 51, pp. 100–114, 2004.
- [8] R. L. Streit and R. F. Barrett, "Frequency line tracking using hidden Markov models," *IEEE Trans. Acoust., Speech, Signal Processing*, vol. 38, pp. 586–598, 1990.
- [9] X. Xie and R. J. Evans, "Multiple target tracking and multiple frequency line tracking using Hidden Markov Models," *IEEE Trans. Sig. Proc.*, vol. 39, pp. 2659–2676, 1991.
- [10] R. F. Barrett and D. A. Holdsworth, "Frequency tracking using hidden Markov models with amplitude and phase information," *IEEE Trans. Sig. Proc.*, vol. 41, pp. 2965–2976, 1993.
- [11] S. Paris and C. Jauffret, "Frequency line tracking using HMM-based schemes," *IEEE Trans. Aerosp. Electron. Syst.*, vol. 39, pp. 439–449, 2003.